JOURNAL OF INDUSTRIAL AND
MANAGEMENT OPTIMIZATION
Volume **3**, Number **3**, August **2007**

Website: http://AIMsciences.org

pp. **585–596**

OPTIMAL CONTROL OF A BATCH CRYSTALLIZATION PROCESS

Volker Rehbock

Western Australian Centre of Excellence in Industrial Optimization
Department of Mathematics and Statistics, Curtin University
of Technology, GPO Box U1987, Perth, WA 6845, Australia

Iztok Livk

Parker Cooperative Research Centre for Integrated Hydrometallurgy Solutions
CSIRO Division of Minerals, PO Box 90, Bentley, WA 6982, Australia

(Communicated by Kok Lay Teo)

Abstract. A dynamic model of an aluminium trihydroxide batch crystallization is considered in this work. The process model, which takes into account kinetics of nucleation, growth and agglomeration, is based on the mass balance of the process and the population balance of the dispersed crystals. Assuming that the temperature of the solution and the seeding policy are variable, optimal control techniques are applied to the model to optimize various performance criteria. Some interesting numerical results for the behaviour of the model are presented.

1. **Introduction.** Crystallization from solution is a purification and separation technique of great economic importance to the chemical industry. The quality of the crystallization product and the efficiency of downstream product recovery processes are primarily determined by the crystal size distribution (CSD). The CSD is thus the main focus in the modelling and optimization of crystallization processes.

In this work, we deal with the precipitation of aluminium trihydroxide ($Al(OH)_3$) from supersaturated sodium aluminate solutions. As part of the Bayer process, it represents an important step in the production of aluminium. In industry practice, the precipitation of aluminium trihydroxide is carried out in a continuous manner using a cascade of crystallizers. For the purpose of a theoretical analysis, however, the complete process can be approximated by a single batch cooling crystallizer. A dynamic model of such a process, based on the mass balance and population balance, was developed in Rawlings *et al* [17]. The concept of population balance modelling of crystallization processes together with crystallization kinetics was first introduced by Randolph and Larson[15]. A discretized form of the population balance, derived later by Marchal *et al* [11] and Hounslow *et al* [3], represents a simple way to compute the crystallization model. Its main advantage is that the agglomeration process can be easily incorporated into the model.

The need for controlled cooling in batch crystallizers has been recognized for a long time and a number of attempts to determine optimal cooling curves can be

2000 *Mathematics Subject Classification.* Primary: 49N90; Secondary: 62P30.
Key words and phrases. optimal control computation, crystallization modelling, Bayer process.

found in the literature. Mullin and Nyvlt [14] proposed that the product CSD can be controlled by programmed cooling. The main idea is to maintain the supersaturation well within the metastable limit where the birth of new crystals is negligible. With this method, the temperature should drop very slowly at the start and become more rapid towards the end of the process in order to grow larger crystals. Similar results were also obtained by applying the maximum principle to the crystallization model (see Jones [8] and Morari [13]). The crystallization kinetics used in these studies were mostly very simplified and the agglomeration process was typically not taken into account.

In this paper, nucleation, growth and agglomeration are all included in the model, making it capable of predicting the entire CSD dynamics. Various performance criteria, such as the final mean size or the amount of fine particles, can be posed to define an optimal control problem which seeks to find an optimal temperature profile and seeding policy (*i.e.* the procedure in which seeding crystals are added during the process). The resulting problem is too complex to be solved via analytical means and we instead employ a numerical optimal control software.

The results presented here may also be of interest to those investigating other types of crystallization processes, as some of the underlying dynamics may be very similar.

2. **Dynamic model of the crystallization process.** Following the approach of Hounslow [3], we discretize the solid particle distribution into m distinct size intervals $[L_i, L_{i+1}]$, $i = 1, \ldots, m$, where size is a measure of the diameter of a particle. A large range of particle sizes can be captured if the L_i are defined by $L_{i+1} = rL_i$, $i = 1, \ldots, m$, where $r = \sqrt[3]{2}$ and $L_1 = 3.7 \times 10^{-6}$ meters. Let N_i denote the number of particles in the i-th size interval. The rate of change of each N_i consists of 3 terms which reflect the effects of nucleation, crystal growth and agglomeration. The nucleation of new particles is assumed to occur only for the first size interval. For the growth, we use the three term expression (equation (43) in Hounslow [3]) as it models the moments of the crystal population quite accurately. The disadvantage of using this expression is that it can lead to undesirable oscillations in the solution of the model. Finally, the agglomeration of particles is modelled by equation (30) of Hounslow [3]. Note that for the first and last size interval, the expressions for growth and agglomeration are altered somewhat to take into account the fact that no particles exist beyond these intervals. The dynamics of the number of crystals in individual size intervals as well as the solute concentration are then described as follows:

$$\frac{dN_1}{dt} = \underbrace{\frac{2G}{L_1(1+r)}\left[\left(1-\frac{r^2}{r^2-1}\right)N_1 - \frac{r}{r^2-1}N_2\right]}_{\text{growth}} + \underbrace{B_u}_{\text{nucleation}} \underbrace{-\beta N_1 \sum_{j=1}^{m} N_j}_{\text{agglomeration}} \quad (1)$$

$$\frac{dN_i}{dt} = \underbrace{\frac{2G}{L_i(1+r)}\left[\frac{r}{r^2-1}N_{i-1} + N_i - \frac{r}{r^2-1}N_{i+1}\right]}_{\text{growth}}$$

$$+\underbrace{\beta\left[N_{i-1}\sum_{j=1}^{i-2}2^{j-i+1}N_j+\frac{1}{2}(N_{i-1})^2-N_i\sum_{j=1}^{i-1}2^{j-i}N_j-N_i\sum_{j=i}^{m}N_j\right]}_{\text{agglomeration}},$$

$$i=2,\ldots,m-1 \tag{2}$$

$$\frac{dN_m}{dt} = \underbrace{\frac{2G}{L_m(1+r)}\left[\frac{r}{r^2-1}N_{m-1}+N_m\right]}_{\text{growth}}$$

$$+\underbrace{\beta\left[N_{m-1}\sum_{j=1}^{m-2}2^{j-m+1}N_j+\frac{1}{2}(N_{m-1})^2-N_m\sum_{j=1}^{m-1}2^{j-m}N_j-\frac{1}{2}(N_m)^2\right]}_{\text{agglomeration}} \tag{3}$$

$$\frac{dC}{dt} = \frac{-3k_v\rho_s}{\varepsilon}G\sum_{i=1}^{m}N_iS_i^2-\frac{\rho_s}{\varepsilon}k_vS_1^3B_u. \tag{4}$$

We consider $m=25$ size intervals, S_i, $i=1,\ldots,m$, denotes the average diameter of particles in the i-th class size, equation (4) models the rate of change of the concentration of the solution if the change of volume is assumed negligible, G is a measure of growth, B_u denotes the rate of nucleation in the first size interval, β is known as the agglomeration kernel (a measure of the frequency of collisions between particles), assumed to be independent of the particle size here, $k_v=0.5$ is a volume shape factor, $\varepsilon=0.8$, and $\rho_s=2420\text{kg/m}^3$ is the density of the resulting solid [9].

Furthermore, letting T denote the temperature of the solution in degrees Kelvin, we can define the solubility as a function of temperature and caustic concentration [12], *i.e.*

$$C^*_{\text{Al}_2\text{O}_3}=C_{\text{Na}_2\text{O}}e^{6.21-\frac{2486.7}{T}+\frac{1.0875C_{\text{Na}_2\text{O}}}{T}},$$

where $C_{\text{Na}_2\text{O}}=100\,\text{kg/m}^3$. The supersaturation, defined as $\Delta C=C-C^*$, is the main driving force for the three processes of nucleation, growth and agglomeration. Following Ilievski and White [4], we model the growth by $G=k_g(\Delta C)^2$, where, assuming $C_{\text{Na}_2\text{O}}=100\text{kg/m}^3$ as before, $k_g=6.2135e^{-\frac{7600}{T}}$ (see Ilievski and White [4]). The dependence of the agglomeration kernel is modelled by $\beta=k_a(\Delta C)^4$, where $k_a=6.8972\times10^{-21}T-2.29\times10^{-18}$ (see Ilievski and White [5] and Li *et al* [10]). According to Ang and Loh [1], the dependence of nucleation on ΔC and T is suitably modelled by

$$B_u=k_n(\Delta C)^{0.8}\left(k_s\sum_{i=1}^{m}N_iS_i^2\right)^{1.7},$$

where $k_s=\pi$ is a surface shape factor and k_n is an empirical coefficient depending on temperature. Note that the above model has been verified with extensive numerical data [9].

Our intended numerical solution method requires all dynamics to be continuously differentiable. The $(\Delta C)^{0.8}$ term in the above equation does not satisfy this criteria as $\Delta C\to0$. Hence, we replace this term by a smooth cubic approximation for small

values of ΔC, *i.e.*

$$B_u = k_n f_c(\Delta C) \left(k_s \sum_{i=1}^{m} N_i S_i^2 \right)^{1.7},$$

where

$$f_c(\Delta C) = \begin{cases} (\Delta C)^{0.8}, & \text{if } \Delta C > 1, \\ -1.2(\Delta C)^3 + 2.2(\Delta C)^2, & \text{if } 0 \le \Delta C < 1. \end{cases}$$

Furthermore, it has been shown experimentally that nucleation decreases markedly at temperatures above 70°C and does not occur beyond 80°C. For temperatures below 70°C, we take $k_n = 9.8 \times 10^{22} e^{\frac{-10407.265}{T}}$, while $k_n = 0$ for temperatures above 80°C. In between, we use a smooth cubic interpolation for k_n, *i.e.*

$$k_n(T) = \begin{cases} 9.8 \times 10^{22} e^{\dfrac{-10407.265}{T}}, & \text{if } T \le 343.2°\text{K}, \\ 151.88834(T-353.2)^3 + 2045.6203(T-353.2)^2, & \text{if } 343.2°\text{K} < T \le 353.2°\text{K}, \\ 0, & \text{if } T > 353.2°\text{K}, \end{cases}$$

where T is measured in degrees Kelvin.

Initially, we shall consider these dynamics over a fixed time interval $[0, t_f]$, but some results will also be obtained for the case of a variable final time t_f. Initial values for the N_i are obtained from a distribution of seeding crystals, *i.e.* crystals added to initialize the crystallization process. To start with, we assume that all seeds are added to the process at $t = 0$. The possibility of having some of the seed at $t = 0$ and adding the remainder in some optimal fashion between $t = 0$ and $t = t_f$ will also be considered. Finally, note that $C(0) = 120\text{kg/m}^3$ throughout.

3. **Optimal control implementation.** We use the software MISER3 [7] to numerically solve the range of problems described below. This code, based on the concept of control parametrization [18], is able to solve a large range of optimal control problems.

We initially assume that only the temperature, T, can be controlled during the process. We choose a piecewise quadratic parametrization for T by modelling its rate of change as a piecewise linear, continuous, function. This allows us to impose constraints on both T itself and on its rate of change. The former constraints are of the continuous state inequality type and can be handled by the method of Jennings and Teo [6].

The optimal control problems to be considered have the form

$$\min_{T} \qquad F$$

subject to the crystallization model and constraints given above. Usually, the aim of the crystallization process is to obtain crystals as large as possible. One way of achieving this goal is to put

$$F = -\ln\left(\frac{M_4}{M_3}\right) = \ln(M_3) - \ln(M_4),$$

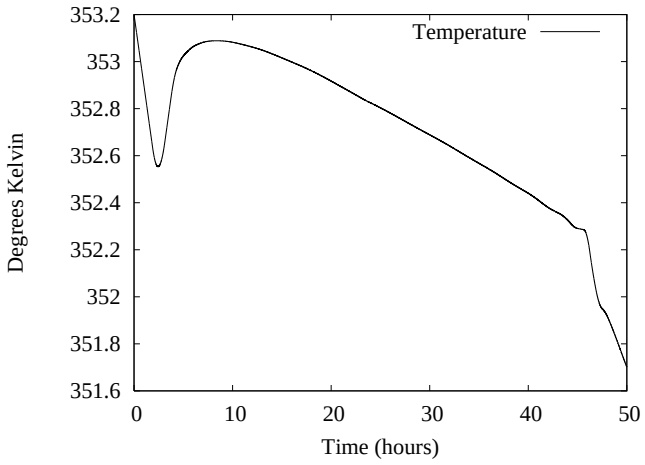

FIGURE 1. Optimal Temperature Profile for Case 1.

where $M_3 = \sum_{i=1}^{m} N_i(t_f) S_i^3$ and $M_4 = \sum_{i=1}^{m} N_i(t_f) S_i^4$ [16]. Minimizing this objective is effectively maximizing the final mean crystal size.

A narrow size distribution, *i.e.* one with a small variance, is also often desired. In this case, one may choose

$$F = -\ln\left(\sqrt{\frac{M_5}{M_4^4} - \frac{1}{M_3 M_4^2}}\right),$$

where $M_5 = \sum_{i=1}^{m} N_i(t_f) S_i^5$ [16]. This is equivalent to maximizing the term

$$\frac{\text{mean crystal size}}{\text{variance}}.$$

We can also consider the case of a variable final time, t_f, for the process. A rescaling of the time horizon and an additional final time constraint are required in this case. We choose to fix the final concentration of the solution, which then defines the yield of the process.

As another variation, we allow a fraction of the seeds to be present in the system at $t = 0$ and then leave the remaining fraction to be added later in the process at a controlled rate. Letting $N_{i,\text{seed}}$ be the number of seeds available in the i-th size interval, we put $N_i(0) = zN_{i,\text{seed}}$, where $0 \le z \le 1$ is variable, and add a term $u(t)N_{i,\text{seed}}$ to the right hand sides of the number balance equations (1)-(3). Here, $u(t)$ represents the rate at which seed crystals are added. To ensure that the total amount of seeds available is not exceeded, we impose the constraint

$$\int_0^{t_f} u(t)\, dt \le 1 - z.$$

Note that this is an inequality constraint which means that it is not necessary to use up all of the seed. All of the variations discussed above can be easily cast into a standard canonical form suitable for solution by MISER3.

For the control functions, two parametrizations, piecewise constant and piecewise linear continuous, are available in MISER3. For the numerical solutions in the next

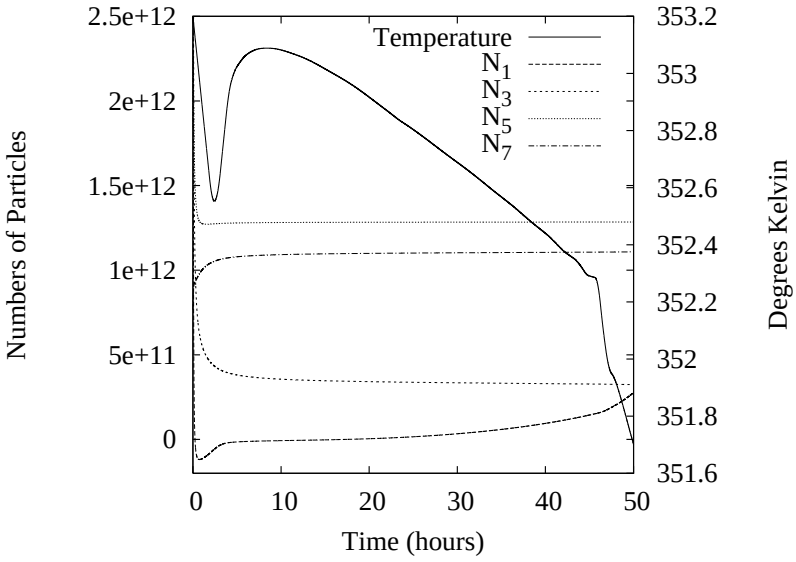

FIGURE 2. Evolution of small particles for Case 1.

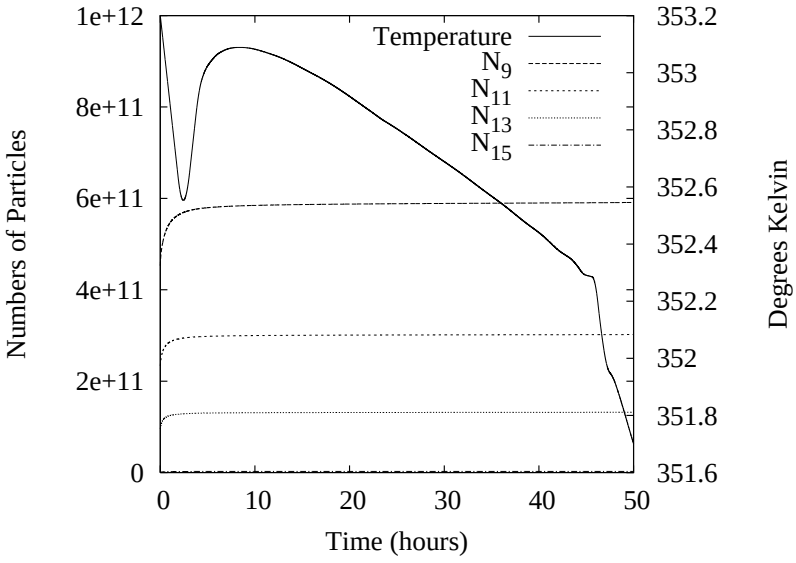

FIGURE 3. Evolution of medium particles for Case 1.

section, we chose a piecewise linear continuous parametrization for both the rate of temperature control (yielding a piecewise quadratic continuous temperature profile) and the seeding policy control.

The resulting problems are quite challenging from a numerical point of view. A particular difficulty is the scale of the state variables, which ranges in values of the order of 10^{13} to order 1. Ideally, N_i, $i = 1, \ldots, m$ should be transformed through use

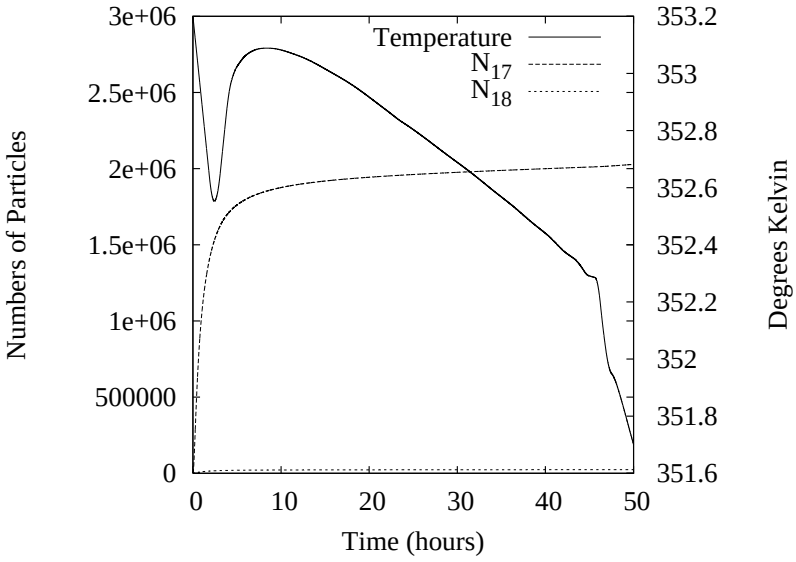

FIGURE 4. Evolution of large particles for Case 1.

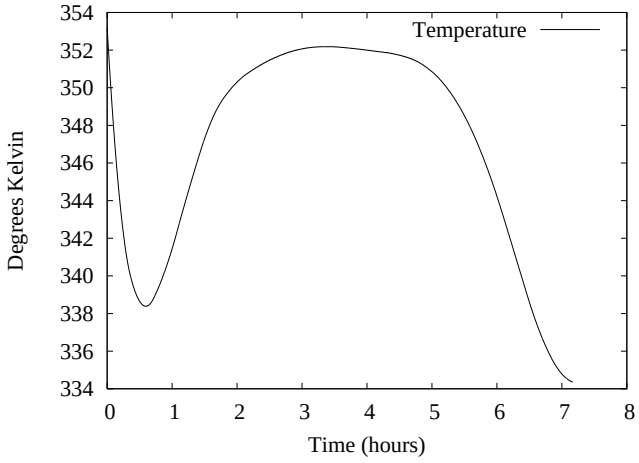

FIGURE 5. Optimal Temperature Profile for Case 2.

of the logarithm function, but the model does allow negative N_i values even though these are not realistic. The dynamics, although poorly scaled, can be integrated by the software if suitably refined partitions for the integration are chosen. We did, however, scale the objective function when it was expressed directly in terms of the numbers of particles (by taking the natural logarithm) to improve the performance of the software.

4. **Numerical results.**

Case 1. Here, $t_f = 50$ hours, $|dT/dt| \leq 0.3$ degrees per hour,

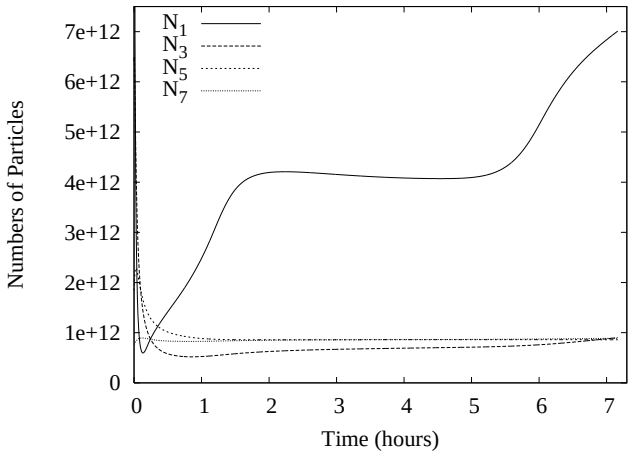

FIGURE 6. Evolution of small particles for Case 2.

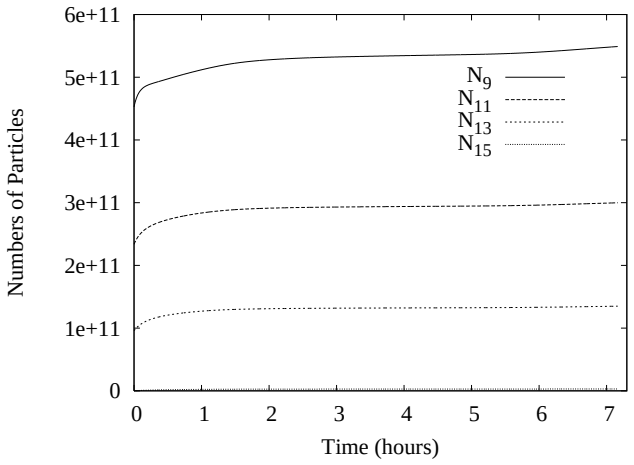

FIGURE 7. Evolution of medium particles for Case 2.

T(0)=353.2°K (=80°C), and our objective is to maximize the final mean crystal size. Note that, in all figures, the horizontal axis shows time in hours. The temperature trajectory presented in Figure 1 shows that, since the rate of change of temperature is tightly constrained, the temperature varies only slightly. The initial dip in the temperature results in the solution being cooled below the metastable limit to encourage nucleation early on. The subsequent temperature profile is aimed at staying close to the maximum temperature to promote crystal growth resulting in an increased final mean crystal size. See [2] for a more thorough explanation of this phenomena. There is a negligible increase in the number of small particles such as those in the N_1 size interval. Figures 2-4 indicates that only a small number of fine particles results in this case. Furthermore, due to a rapid crystal growth at high temperatures, mean crystal size is being increased.

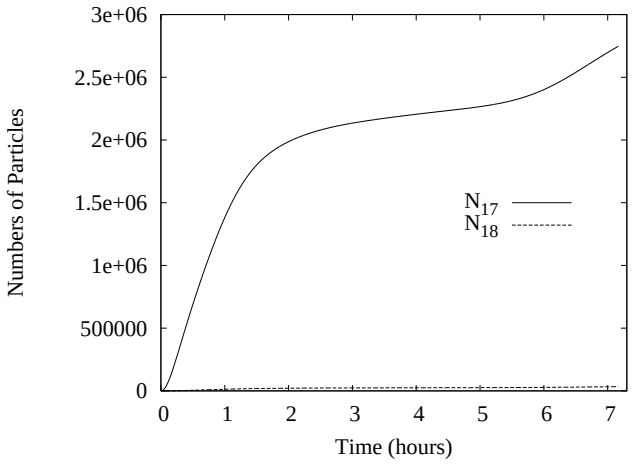

FIGURE 8. Evolution of large particles for Case 2.

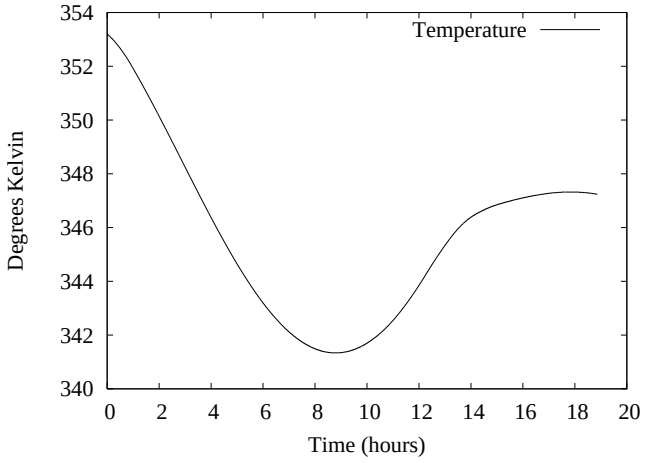

FIGURE 9. Optimal Temperature Profile for Case 3.

Case 2. We now impose the constraint $C(t_f) = 55\,\mathrm{kg/m^3}$ and allow t_f to be variable. The objective here is to maximize the mean size of the final crystal population divided by its variance. To explore some of the more interesting behaviour of the model, we relax the constraints on temperature, choosing $|dT/dt| \leq 60$ degrees per hour. Figure 5 shows that in order to promote agglomeration and consequently produce larger particles, the temperature of a crystallizing system should be lowered rapidly at the beginning of a process. This will take the solution below the metastable limit and promote nucleation early on, as discussed in Case 1. Then, however, the temperature should be raised again to avoid excessive nucleation. Towards the end of the process, the temperature should be lowered to reach the desired product yield imposed by the terminal concentration constraint. Compared to Case 1, while the number of fine particles has increased (see Figure 6) we also obtain a

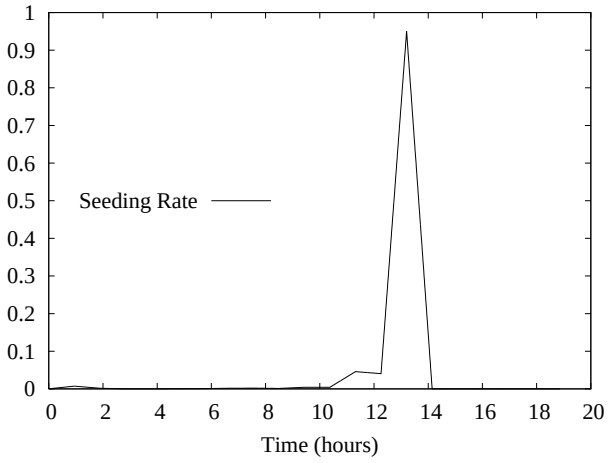

FIGURE 10. Optimal Seeding Strategy for Case 3.

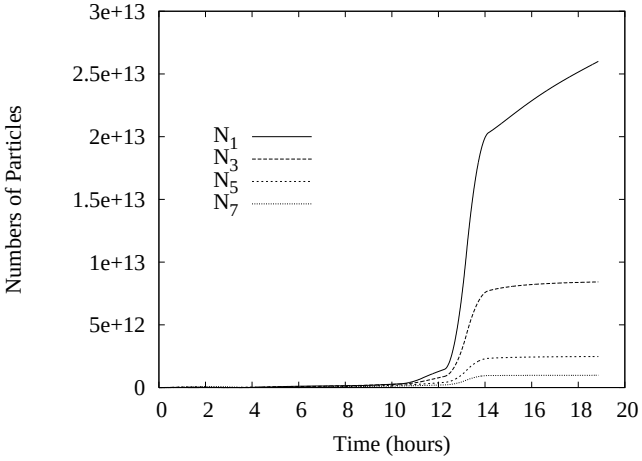

FIGURE 11. Evolution of small particles for Case 3.

larger final mean size here. This can be explained by a significant increase in the number of large particles, also shown in Figure 8 and by the increased overall yield forced on the model by the additional terminal concentration constraint.

Case 3. Here we add the variable seeding policy discussed in the previous section. Again, there are essentially no constraints on temperature. Note that with the same objective as in Case 2, the seeding strategy remains unchanged, with all seed added at the start of the process and none later. However, we get very different results if the objective is changed to one of maximizing the total number of particles in the first seven size intervals (*i.e.* $F = -\ln(N_1 + N_2 + N_3 + N_4 + N_5 + N_6 + N_7)$). As shown in Figures 9 and 10, the optimal temperature profile suggests that in the first stage the solution should be cooled by some 12°C and then the seed introduced.

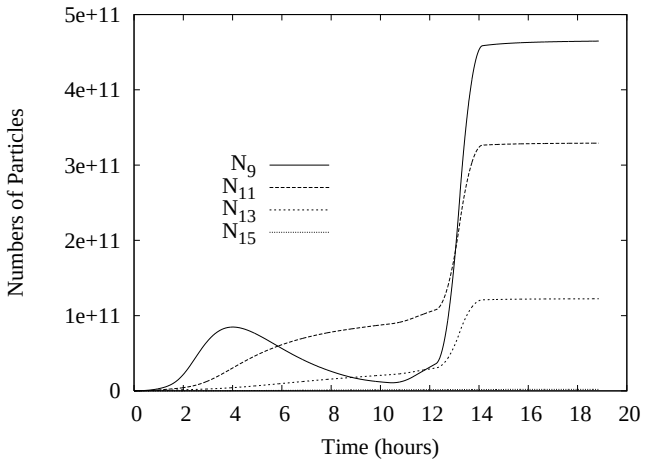

FIGURE 12. Evolution of medium particles for Case 3.

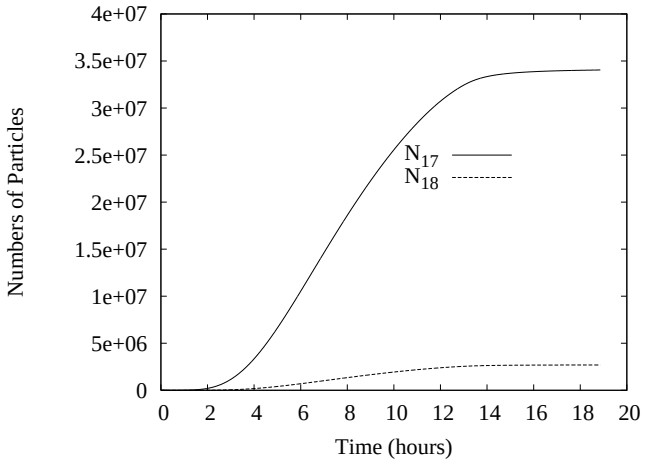

FIGURE 13. Evolution of large particles for Case 3.

After all the seed has been added the temperature is kept almost constant. The resulting profiles for various particle size intervals are also shown in Figures 11-13.

5. **Conclusions.** In this paper we investigated the numerical optimization of a batch crystallization process. A dynamic model considered in this work includes kinetics of the nucleation, growth and agglomeration processes. Using different objective functions we showed that optimal temperature profiles obtained for our model differ significantly from those obtained previously for more simplified systems. It was also shown that in some cases the seeding policy can considerably affect the final product quality. Finally, it should be noted that some of the objective functions investigated in this work are not very sensitive to the temperature profile. Future work in this area will concentrate on modified objective functions which

better reflect industry needs and more accurate dynamic models such as those incorporating a size dependent agglomeration kernel, for example.

Acknowledgements. We thank the anonymous referees for their suggestions which have greatly improved the presentation of the paper.

REFERENCES

[1] H.M. Ang and P.I.W. Loh, *Kinetics of secondary nucleation of alumina trihydrate in a batch crystallizer*, in "Crystalization as a Separation Process" (eds. A.S. Myerson and K.T. Toyokura), American Chemical Society Symposium Series, 1990, 329–343.

[2] M.J. Hounslow and G.K. Reynolds, *Product engineering for crystal size distribution*, AIChE Journal, **52** (2006), 2507–2517.

[3] M.J. Hounslow, R.L. Ryall and V.R. Marshall, *A discretized population balance for nucleation, growth and aggregation*, AIChE Journal, **34** (1988), 1821–1832.

[4] D. Ilievski and E.T. White, *Agglomeration during precipitation: Agglomeration mechanism identification for $Al(OH)_3$ crystals in stirred caustic aluminate solutions*, Chem. Eng. Sci., **49** (1994), 3227–3239.

[5] D. Ilievski and E.T. White, "Modelling Bayer Precipitation with Agglomeration," Light Metals 1995, Las Vegas, NV, Warrendale, PA: The Minerals, Metals and Materials Society, (1994), 55–61.

[6] L.S. Jennings and K.L. Teo, *A computational algorithm for functional inequality constrained optimization problems*, Automatica, **26** (1990), 371–375.

[7] L.S. Jennings, M.E. Fisher, K.L. Teo and C.J. Goh, *MISER3: Solving optimal control problems*, Advances in Engineering Software, **13** (1991), 190–196.

[8] A.G. Jones, *Optimal operation of a batch cooling crystallizer*, Chem. Eng. Sci., **29** (1974), 1075–1087.

[9] T.S. Li, I. Livk and D. Ilievski, *The influence of crystallizer configuration and on the accuracy and precision of gibbsite crystallization kinetics estimates*, Chem. Eng. Sci., **56** (2001), 2511–2519.

[10] T.S. Li, I. Livk and D. Ilievski, *Supersaturation and temperature dependency of gibbsite growth in laminar and turbulent flows*, Journal of Crystal Growth, **258** (2003), 409–419.

[11] P. Marchal, R. David, J.P. Klein and J. Villermaux, *Crystallization and precipitation engineering - I. An efficient method for solving population balance in crystallization with agglomeration*, Chem. Eng. Sci., **43** (1988), 59–67.

[12] C. Misra and E.T. White, *Kinetics of crystallization of aluminium trihydroxide from seeded caustic aluminate solutions*, Chemical Engineering Progress Symposium Series, **67(110)** (1971), 53–65.

[13] M. Morari, *Some comments on the optimal operation of batch crystallizers*, Chemical Engineering Communications, **4** (1980), 167–171.

[14] J.W. Mullin and J. Nyvlt, *Programmed cooling of batch crystallizers*, Chem. Eng. Sci., **26** (1971), 369–377.

[15] A.D. Randolph and M.A. Larson, "Theory of Particulate Processes," Academic Press, New York, 1971.

[16] A.D. Randolph and M.A. Larson, "Theory of Particulate Processes: Analysis and Techniques of Continuous Crystallization," 2nd ed. Academic Press, Toronto, 1988.

[17] J.B. Rawlings, S.M. Miller and W.R. Witkowski, *Model identification and control of solution crystallization processes: a review*, Ind. Eng. Chem. Res., **32** (1993), 1275–1296.

[18] K.L. Teo, C.J. Goh and K.H. Wong, "A Unified Computational Approach for Optimal Control Problem," Longman, Essex, 1991.

Received November 2005; 1st revision February 2007; 2nd revision May 2007.

E-mail address: V.Rehbock@curtin.edu.au
E-mail address: Iztok.Livk@csiro.au